Stanford Exploration Project, Report 89, November 12, 1997, pages 181–193

Linearized elastic inversion in the $k - \omega$ domain

Giancarlo Bernasconi[1], *Giuseppe Drufuca*[2], *Fabio Rocca*[2]

keywords: *inversion, modeling, elastic, Fourier transform, algorithm, estimation*

ABSTRACT

We present an algorithm for elastic linearized inversion in the wavenumber-frequency domain. The medium is considered to be composed of a known constant background plus an unknown small variation of P-impedance, S-impedance and density. The linearized approach enables us to use the tools of linear algebra to analyze the ill-conditioning of the inversion. Operating in the wavenumber-frequency domain, we gain the advantage of the simplicity of the theory, as the scattering process becomes the interaction of monochromatic plane waves with sinusoidal variations of the elastic parameters. Inversion and analysis of the information give a smoothed but reliable image of the original model. We test the algorithm on synthetic data. Because of the ill-conditioning of the inverse problem, we find that even small numerical errors cause deterioration of the quality of inversion: P-P reflections allow an accurate estimation of P-impedance perturbation only. Multicomponent data are necessary to recover S-impedance perturbation with this approach.

INTRODUCTION

Seismic inversion is aimed at giving a detailed description of the earth's rock physics. In this paper we explore the implementation aspects of the elastic linearized inversion in the k–ω domain introduced by Rocca and De Nicolao (1993).

The chosen elastic parameters are P-impedance, S-impedance and density. The medium is considered to be composed of a known constant background plus an unknown small variation of the elastic parameters. The hypothesis of small contrasts enables us to use the Born approximation and to linearize the scattering properties of point diffractors (Wu and Aki, 1985). The formulation is similar to that developed in Clayton and Stolt (1981) and Miller et al. (1987) for the acoustic case. The extension to the elastic case is done by expressing the reflectivity term as a linear function of elastic perturbations (Stolt and Weglein, 1985, Beydoun and Mendes, 1989, De

[1]**email**: bernasco@elet.polimi.it
[2]Dip. di Elettronica e Informazione, POLIMI, Italy.

Nicolao et al., 1993).

We plan to insert the algorithm in a target-oriented inversion scheme, so limiting its application to a restricted zone of the subsurface, where the hypothesis of small variations of the parameters holds. For a realistic earth model, we must assume that the target is embedded in a complex stratified or inhomogeneous overburden, which has propagation effects such as geometrical spreading, transmission coefficients across elastic interfaces, anisotropy, wavefront distortion, multiples. If the overburden parameters are known, its effects can be removed from the inversion problem by a downward continuation (datuming) of sources and receivers to the target location. Our current work, not included in this paper, involves the development of a datuming scheme in the k–ω domain (Bernasconi et al., 1995). Moreover, a target-oriented approach is well suited for 3D geometries, as we can concentrate the computing resources on a small part of the model. In this paper we consider 2D media, but the extension to 3D media is straightforward.

Operating in the k–ω domain, we gain the additional advantage of the simplicity of the theory: perturbations of a uniform background are decomposed in sinusoidal components. The Bragg resonance condition (Born and Wolf, 1959) links plane monochromatic incident and reflected waves to the medium wavenumber, so we obtain a simple relation between data and parameters. The inversion can be done separately for each point of the model spectrum (k domain), so we deal with small matrices. In practice we collect the contributions to the reflected field of one sinusoidal component at a time.

Inversion and analysis of the information is achieved by means of singular value decomposition of the data-model relation and least-squares estimation along the eigenvectors. In this way, we obtain a robust, fast and efficient algorithm. The recovered model is a "filtered" but reliable version of the original model, as it contains only and all the information that we can extract from the data.

The ill conditioning of the inverse problem (De Nicolao et al. 1993) does not allow a good estimation of all three elastic parameters. Even small numerical errors can cause the quality of inversion to deteriorate and produce interference between parameter estimates. Similar effects result from the practical aspects of data collection and processing. Truncations due to the finite length of the cable, the finite number of sources and receivers, and the limited bandwidth of the wavelet produce aliasing and a distorted reconstruction of the original model. The main consequence is that P-P reflections allow an accurate estimation of P-impedance perturbation only. To recover S-impedance perturbation we must use multicomponent data, namely P-SV reflections. We demonstrate this with synthetic data. Particular care is taken in the choice of the processing sequence that minimizes the disturbances.

Although not investigated in this paper, we think that an improvement of the results can be achieved adding some a priori information (interpretative inversion). If we impose boundaries to the variations of the elastic parameters, we reduce the null space and the indetermination of the inversion.

THE ALGORITHM

From data to model space

We follow the procedure outlined by Bernasconi et al. (1994). P-wave isotropic point sources and receivers are located on the surface of a medium characterized by small 2D deviations of the elastic parameters from a known uniform background. We compute synthetic seismograms using the linearized scatter patterns of a point diffractor (Wu and Aki, 1985) and the Born approximation: small reflection coefficients make multiple reflections negligible. The reflectivity is expressed as a linear combination of elastic perturbations. The chosen parameter set is P-impedance relative perturbations $\Delta Ip/Ip$, S-impedance relative perturbations $\Delta Is/Is$ and density relative perturbations $\Delta\rho/\rho$. The input data is a set of common shot gathers. They form a cube (data space) whose axes are

- t time,
- x_s source coordinate,
- x_h offset coordinate.

A Fourier transformation over source and offset coordinate leads to a cube in the domain

- t time,
- k_s source wavenumber,
- k_h offset wavenumber.

Transformation to the (ω, k_x, k_z) domain (model domain) is accomplished through diffraction tomography techniques (Wu and Toksö, 1987). To illustrate the basic principle of diffraction tomography we consider an infinite medium and an incident monochromatic plane wave with wavenumber $\mathbf{k}_i$. The reflected plane wave $\mathbf{k}_r$ depends upon only one Fourier component of the medium (Figure 1).

Let $\mathbf{k}_m$ be the vector of medium wavenumbers (k_x, k_z). The relation between the medium wavenumber and the incident and reflected waves is

$$\mathbf{k}_m = \mathbf{k}_r - \mathbf{k}_i. \tag{1}$$

A reflected plane wave due to an incident plane wave illuminates only one point in the model space (k_x, k_z): this is a Bragg resonance effect. Therefore the mapping of data space (t, k_s, k_h) into the model space (ω, k_x, k_z) is

$$k_x = k_s, \tag{2}$$

$$k_z = \sqrt{\left(\frac{\omega}{v_r}\right)^2 - k_h^2} + \sqrt{\left(\frac{\omega}{v_i}\right)^2 - (k_h - k_s)^2}, \tag{3}$$

where v_r and v_i are the velocities of the reflected and incident waves, respectively.

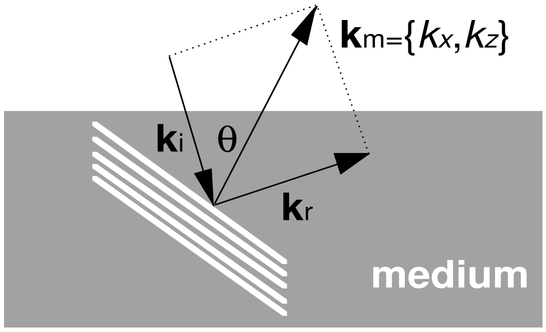

Figure 1: Diffraction Tomography: the Bragg effect. A reflected and an incident monochromatic plane wave enlighten only one sinusoidal component of the medium. giancarlo-diff-tomog [NR]

Given k_x and k_z, we solve equations (2) and (3) to obtain a value of ω for each value of k_h. The data are migrated through a t–ω transform. The t–ω transform is evaluated with a DFT. This operation is performed one point at a time in the (k_x, k_z) domain, so we collect the contributions to the reflected field of a single sinusoidal perturbations at a time.

Spectral coverage is affected by cable length (angular aperture) and finite bandwidth. With surface acquisition, the horizontal wavenumbers are not recoverable (Figures 2 and 3) as they fall in the non-observable part of the spectrum (null space).

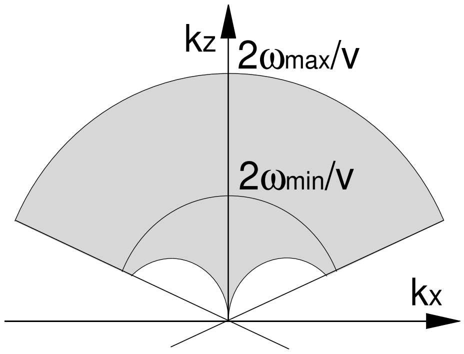

Figure 2: Coverage of the model spectrum with surface acquisition and limited bandwidth from ω_{min} to ω_{max} (Wu and Toksöz, 1987). The angular aperture is linked to the the maximun observation angle. The background velocity is v. giancarlo-kxkz-domain [NR]

Inversion

It is important to notice that a point (ω, k_s, k_h) in data space fixes the angle θ of the incident plane wave as well. Because of the Bragg condition, the ω dependence in model space is transformed into incidence-angle dependence, according to

$$\cos\theta = \frac{(\frac{\omega}{v_i})^2 - (\frac{\omega}{v_o})^2 + k_x^2 + k_z^2}{2\frac{\omega}{v_i}\sqrt{k_x^2 + k_z^2}}. \tag{4}$$

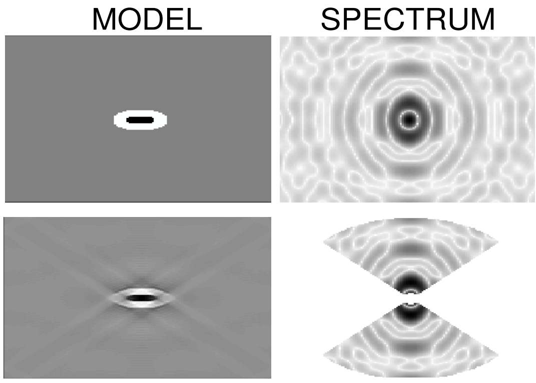

Figure 3: Effects of the limited angular aperture and bandwidth on the spectrum and on the model. Horizontal variations in the model are unrecoverable with surface acquisition as they fall in the non-observable part of the spectrum. giancarlo-mod-spec [NR]

For each point in the (k_x, k_z) domain, that is for each sinusoidal component in the space domain, the θ dependence is a vector $\mathbf{d}(\theta)$. This represents the Phase versus Angle (PvA) and Amplitude versus Angle (AvA) of the sinusoidal component of the medium (Figure 4),

$$\mathbf{d}(\theta) = \mathbf{G}(\theta)\ \mathbf{m}, \tag{5}$$

with $\mathbf{m} = [\Delta Ip/Ip\ ,\ \Delta Is/Is\ ,\ \Delta\rho/\rho]$.

The matrix $\mathbf{G}$ describes the reflection angle dependence, the wavelet spectrum, the propagation effects and the directivity of sources and receivers. Figure (5) illustrates the reflection coefficient of a sinusoidal medium due to unitary parameter perturbations for P-P and P-SV reflections.

The inversion is a least-squares fit of the measured PvA and AvA, which is the result of the mapping process, with the theoretical PvA and AvA in the complex plane. We use the SVD decomposition of the relation data-parameters $\mathbf{G} = \mathbf{U}\mathbf{\Lambda}\mathbf{V}^T$ (Lines and Treitel 1984). The matrix $\mathbf{U}$ contains the eigenvectors in data space. $\mathbf{\Lambda}$ is the diagonal matrix of singular values. They represent the energy in the data due to a unitary variation along eigenvectors axis in the model space. $\mathbf{V}$ contains the eigenvectors in model space: they form an orthogonal basis in the model space and are linear combinations of the elastic parameters perturbations $\Delta Ip/Ip$, $\Delta Is/Is$ and $\Delta\rho/\rho$.

The reflections of each sinusoidal component are inverted one by one: given (k_x, k_z) and the corresponding migrated data $\mathbf{d}_m(\theta)$,

$$\mathbf{m} \simeq \mathbf{V}\ \mathbf{\Lambda}^{-1}\mathbf{U}^T\mathbf{d}_m. \tag{6}$$

The data $\mathbf{d}_m(\theta)$, plotted in the complex plane, form a line (Figure 4). The inclination of the line gives the phase of the sinusoidal component. The absolute value of the data is the measured AvA of the sinusoidal medium.

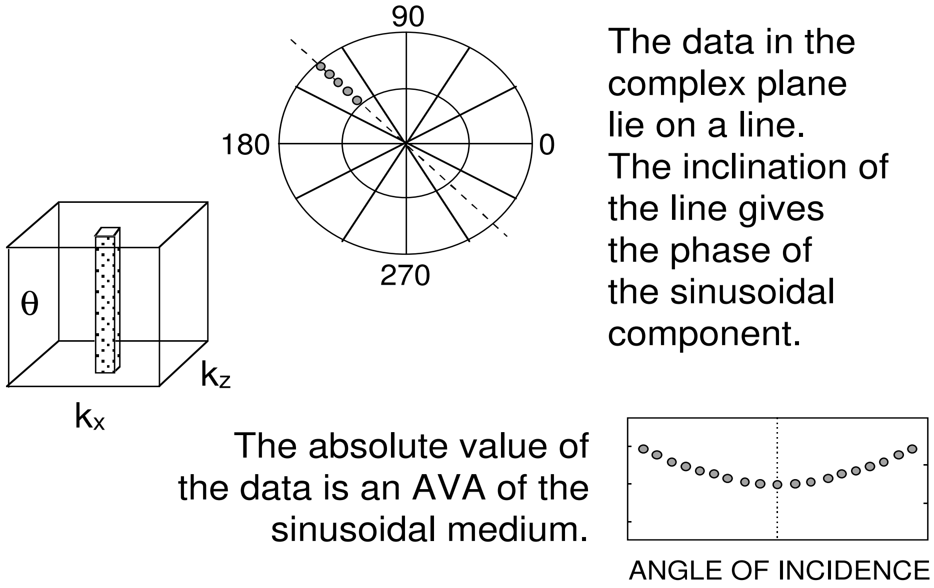

Figure 4: Interpretation of $\mathbf{d}(\theta)$ for a given (k_x, k_z). giancarlo-PvA-AvA [NR]

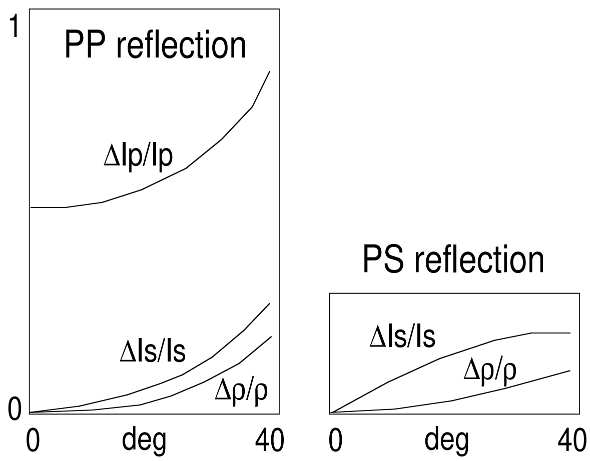

Figure 5: Theoretical AvA of a sinusoidal medium for a unitary change of parameters. giancarlo-unitary [NR]

Because of the finite range of sources, receivers, frequency components and observation angles, only a part of the entire model spectrum can be recovered. Non-observable components of the spectrum (null space) are not inverted. Sharp transitions of the angular coverage in the (k_x, k_z) domain are tapered before transformation to the x–z panels.

The ill-conditioning of the inverse elastic problem can lead, because of the presence of numerical inaccuracies and interpolation errors, to interference between parameters estimates. De Nicolao et al. (1993) have found that with realistic signal-to-noise-ratios, in this linearized approach, P-P reflections allow an accurate estimation of P-impedance perturbation only. S-impedance perturbation can be recovered with multicomponent data, namely P-SV reflections. Density perturbations are practically unrecoverable. We have tested these results on synthetic examples, which are described below.

EXAMPLES

The first model is a single sinusoidal perturbation of P-impedance (Figure 6). In the transformed domain, it is represented by an impulse, broadened because of the windowing in the spatial domain. The data are synthetic seismograms for P-P reflections. Figure (6) shows the AvA and the PvA extracted from the data in the transformed domain for the point corresponding to the sinusoidal medium. They are compared with the theoretical AvA and PvA. The small unavoidable numerical errors (less than 3%) cause leakage from $\Delta Ip/Ip$ to $\Delta Is/Is$ and $\Delta\rho/\rho$. Consequently, the estimate of S-impedance and density from P-P reflections is unreliable even with synthetic data.

The second model (Figure 7) mimics a fault with a gas-bearing sand target in the upper part, where P-impedance and S-impedance variations occur.

We have evaluated synthetic common shot gathers for P-P and P-SV reflections; some gathers are shown in Figure 8. The position of the source is indicated by a star. Acquisition geometry is reported in Figure 7.

Inversion of P-P data allows an accurate reconstruction of P-impedance perturbation (Figure 9). Due to the limited observation angle, horizontal variations cannot be recovered. We have increased the maximun incident angle by doubling the cable length. The inversion gives similar results (Figure 9, right): P-impedance estimation is mainly governed by normal incidence.

S-impedance inversion from P-P data is masked by P-impedance leakage (Figure 10). If we use P-SV data, S-impedance perturbation is correctly recovered (Figure 11). The accuracy increases by doubling the cable length. In fact, for normal incidence, the P-SV reflection coefficient vanishes (Figure 5): S-impedance estimation improves with higher incident angles.

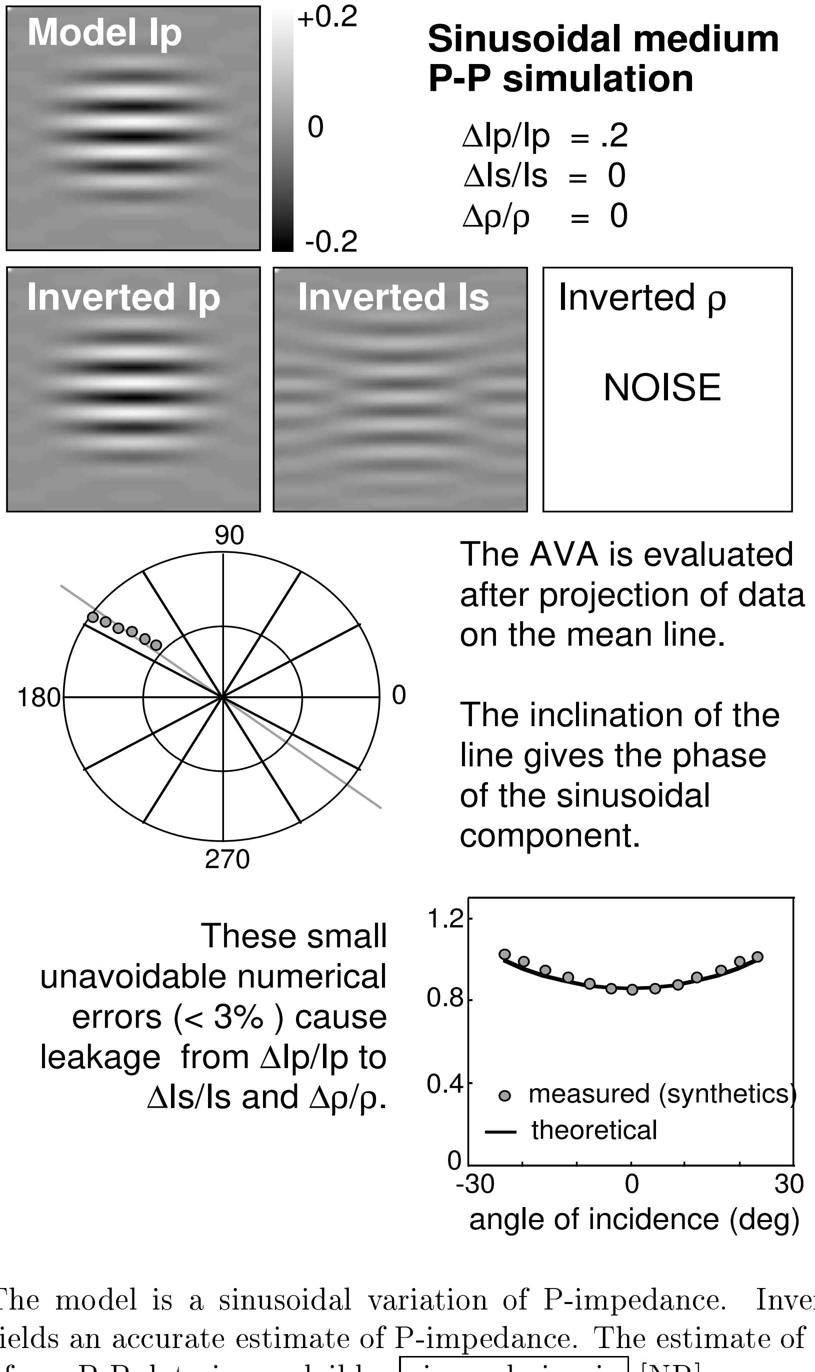

Figure 6: The model is a sinusoidal variation of P-impedance. Inversion of P-P reflections yields an accurate estimate of P-impedance. The estimate of S-impedance and density from P-P data is unrelaible. $\boxed{\text{giancarlo-invsin}}$ [NR]

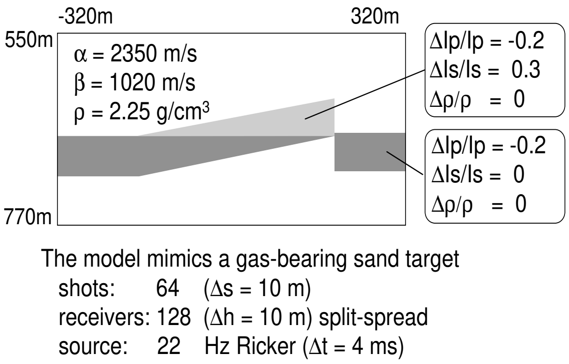

Figure 7: Model and acquisition parameters. giancarlo-fault [NR]

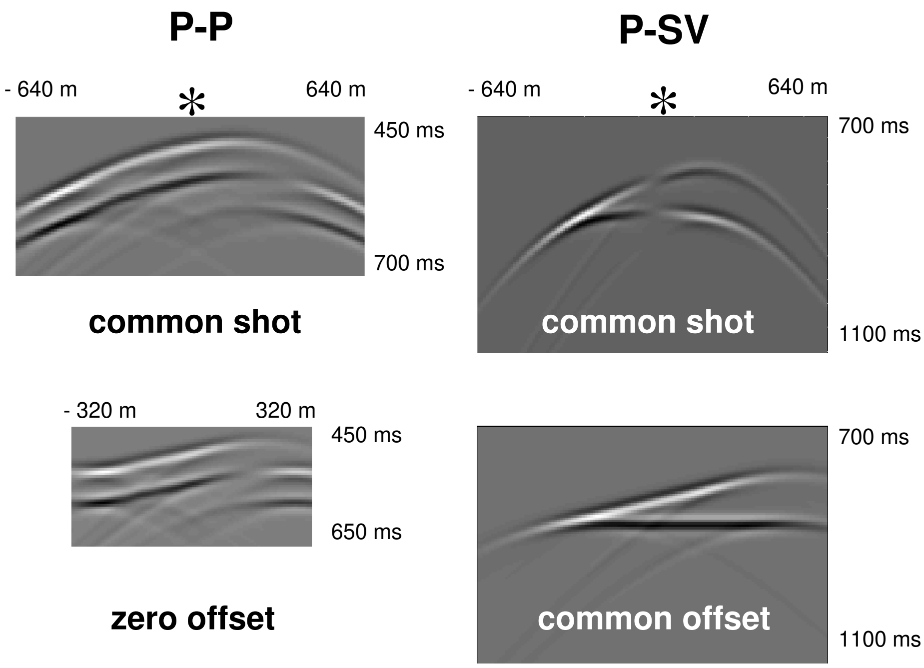

Figure 8: Synthetic gathers. The model is shown in Figure 7. giancarlo-gathers [NR]

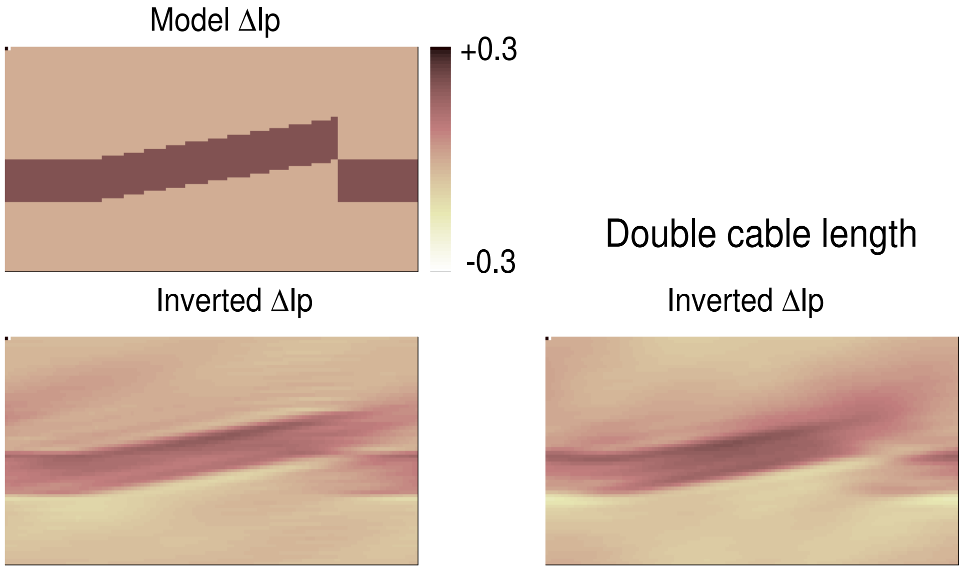

Figure 9: Inversion of $\Delta Ip/Ip$ from P-P data. $\Delta Ip/Ip$ is recovered. giancarlo-invIp-PP [NR]

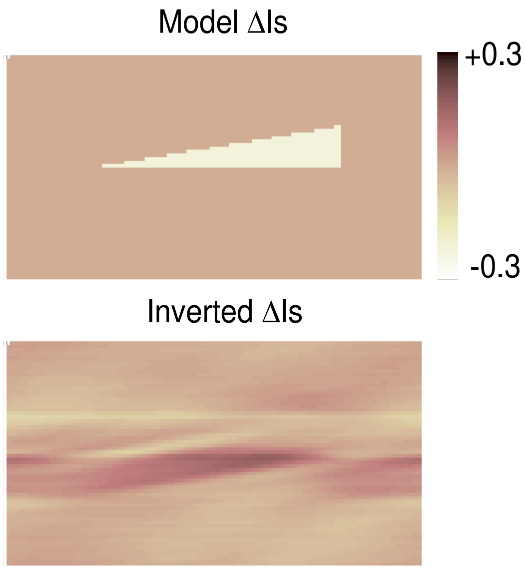

Figure 10: Inversion of $\Delta Is/Is$ from P-P data. Recovered $\Delta Is/Is$ is masked by leakage from $\Delta Ip/Ip$. giancarlo-invIs-PP [NR]

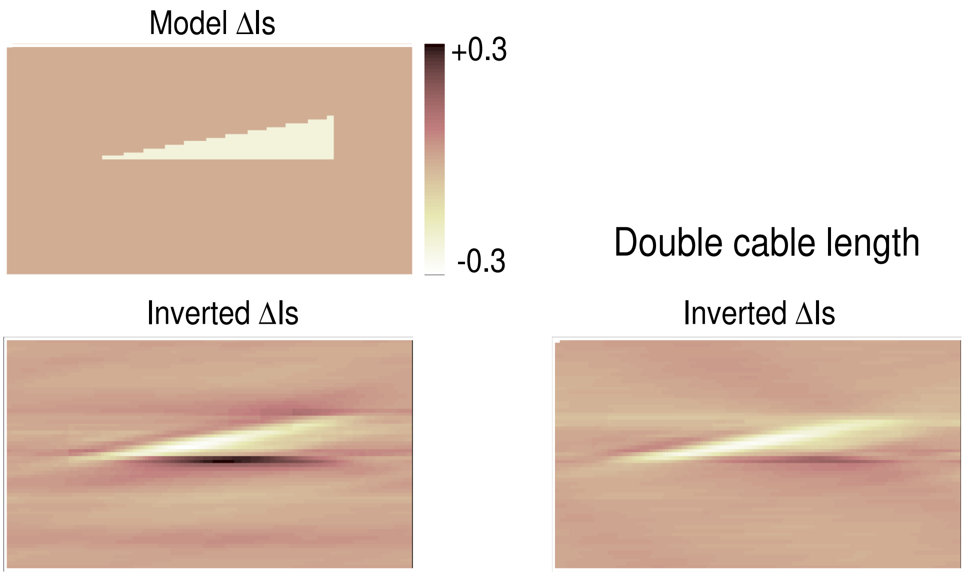

Figure 11: Inversion of $\Delta Is/Is$ from P-SV data. $\Delta Is/Is$ is recovered. giancarlo-invIs-PS [NR]

CONCLUSIONS

We have developed an algorithm for elastic seismic inversion in the k–ω domain. domain. It uses diffraction tomography techniques and DFT interpolation to map the data space into the model space. The linearized k–ω approach allows to analyze the inverse problem and to control the indeterminations due to the geometry of acquisition (finite bandwidth and cable length). The algorithm is fast and efficient.

Tests on synthetic data have shown that, even in this ideal case, the ill conditioning of the inverse problem does not allow the estimation of all the elastic parameters. The inversion of P-P reflections produces an accurate estimate of P-impedance perturbation only. S-impedance perturbation can be recovered with multicomponent data.
Our future work will address
- inclusion of the algorithm in a target-oriented inversion scheme, adding the treatment of stratigraphic overburdens;
- application to real data;
- extension to 3D media.

ACKNOWLEDGEMENTS

This research is sponsored by CEC within the framework of the GEOSCIENCE II Program, Contract JOU2-CT92-0096. GB thanks SEP for hosting him during summer 1995.

REFERENCES

Bernasconi, G., Drufuca, G., Rocca, F., 1994, Linearized elastic inversion in the k–ω domain: 64th Internat. Mtg. Soc. Expl. Geophys., Expanded Abstracts.

Bernasconi, G., Drufuca, G., Rocca, F., 1995, Datuming for target oriented inversion in the k–ω domain: 57th Internat. Mtg. Eur. Assoc. Expl. Geophys., Expanded Abstracts.

Beydoun, W., Mendes, M., 1989, Elastic ray-Born l_2-migration/inversion: Geophysical Journal, **97**, 151-160.

Born, M., Wolf, E., 1959. Principles of optics; electromagnetic theory of propagation, interference and diffraction of light: Pergamon Press.

Clayton, R. W., Stolt, R. H., 1981, A Born-WKBJ inversion method for acoustic reflection data: Geophysics, **46**, 1559-1567.

De Nicolao, A., Drufuca, G., Rocca, F., 1993, Eigenvalues and eigenvectors of linearized elastic inversion: Geophysics, **58**, 670–679.

Lines, L. R., Treitel, S., 1984. Tutorial. A review of least-squares inversion and its applications to geophysical problems: Geophysical Prospecting, **32**, 159–186.

Miller, D., Oristaglio, M., Beylkin, G., 1987, A new slant on seismic imaging: Migration and integral geometry: Geophysics, **52**, 943–964.

Rocca, F., De Nicolao, A., 1993, Linearized elastic inversion in the k–ω domain: 55th Mtg. Eur. Assoc. Expl Geophys., Expanded Abstracts.

Stolt, R. H., Weglein, A. B., 1985. Migration and inversion of seismic data: Geophysics, **50**, 2458–2472.

Wu, R. S., and Aki, K., 1985, Scattering characteristics of elastic waves by an elastic heterogeneity: Geophysics, **50**, 582–595.

Wu, R. S., and Toksöz, M. N., 1987, Diffraction tomography and multisource holography applied to seismic imaging: Geophysics, **52**, 11–25.